This is the accepted manuscript (postprint) of the following article:
Bahari-Sambran, F., Meuchelboeck, J., Kazemi-Khasragh, E., Eslami-Farsani, R., & Chirani, S. A. (2019). The effect of surface modified nanoclay on the interfacial and mechanical properties of basalt fiber metal laminates. *Thin-Walled Structures*, *144*, 106343.
https://doi.org/10.1016/j.tws.2019.106343

The effect of surface modified nanoclay on the interfacial and mechanical properties of basalt fibers metal laminates

F. Bahari-Sambran[1], J. Meuchelboeck[2], E. Kazemi-Khasragh[1], R. Eslami-Farsani[1]*, S. Arbab Chirani[3]

[1]*Faculty of Materials Science and Engineering, K. N. Toosi University of Technology, No. 7, Pardis St., Mollasadra Ave., Vanak Sq., Tehran, Iran*

[2]*Faculty of Engineering Science, University of Bayreuth, University Street 30, 95447 Bayreuth, Germany*

[3]*ENI Brest, FRE CNRS 3744, IRDL, Brest, France*

*Corresponding author: eslami@kntu.ac.ir

Abstract

In this study, the effect of different percentages of modified nanoclay (1, 3, and 5 wt.%) on the mechanical behavior of fibers metal laminates (FMLs) made up of aluminum and basalt fibers-epoxy composite was investigated. The surface treatment was conducted on aluminum in order to obtain a proper adhesion between aluminum and epoxy. The Charpy test results showed that the absorbed energy values of the samples containing nanoclay were increased compared to the samples without nanoclay. Improving the impact strength of FMLs containing nanoclay was due to the enhancement of the basalt fibers/epoxy interfacial properties and creating some physical entanglement such as mechanical interlocking between the polymer chains and nanoclay. Otherwise, nanoclay addition decreased the interlaminar shear strength of FMLs. The microscopic images of aluminum debonding surfaces revealed that the agglomerated nanoclay particles prevent the epoxy infiltration into porous structures of aluminum layer and consequently, weaken the interlaminar shear strength.

Keywords: Fiber metal laminates, Basalt fibers, Nanoclay, Charpy test, Interlaminar shear strength.

1. Introduction

During the recent years, the application of composite materials has been developed in the automotive field and in anywhere that the light-weight components are demanded. Combining the properties of both metals and polymeric composites was the main reason for the development of hybrid materials made from thin metallic sheets and fiber-reinforced polymers. Fiber metal laminates (FMLs) are a type of hybrid composites based on alternating layers of fiber reinforced polymers and metal sheets [1-5]. The most common metals that can be used in FMLs are aluminum, titanium, and magnesium. In addition, carbon, glass, and Kevlar are the most extensively used fibers in the composite core of FMLs [6]. In fact, combining the stability and plastic behavior of metallic laminates with the high fatigue resistance of composite materials is the initial purpose for the production of FMLs. Moreover, the low fatigue resistance of aluminum alloys can be enhanced using the FMLs [7]. FMLs show such enhanced properties as high specific strength/stiffness, good fatigue resistance, fracture toughness, and a high capacity of energy absorption [8, 9].

The fracture and fatigue behavior of FMLs are greatly affected by shear stresses/strength. Shear stresses and the shear strength both inter and intralaminar have an important role in the fracture and fatigue behavior of FMLs. When the composite is subjected to interlaminar shear stresses (e.g. bending moments), the relatively low shear strength can contribute to interlaminar failure [10]. The short-beam shear (SBS) test is the chief method for determining the interlaminar shear strength (ILSS) of FMLs laminates since this method is characterized by simplicity and feasibility [11]. Liu et al. [11] investigated the interlaminar failure behavior of GLARE laminates under short-beam three-point-bending load with various span length-to-specimen thickness ratios (L/h). They reported that a valid shear dominant failure mode was obtained at the L/h ratio of 8.

Basalt fibers are known as mineral fibers which are obtained from volcanic rocks [12]. Basalt fibers show several advantages such as excellent adhesion to the resin, good resistance to chemical attack, low water absorption, sound insulation, and high-temperature functioning range. Moreover, basalt fibers have attracted more attention due to their availability, economic cost, and ease of production. In the case of mechanical properties, basalt fibers present higher fracture strain and tensile strength in comparison with carbon fibers and glass fibers, respectively. The symbiosis of conventional reinforcements such as fibers and nanofillers produces the multi-scaling composites and can result in polymer composites with enhanced properties [13-17].

Due to low cost, lightweight, high strength, and easy processing, epoxy nanocomposites are being used for different applications in various industries [18, 19]. The positive effect of multi-walled carbon nanotubes on impact behavior [20, 21] and ILSS properties [22] of FMLs has been proved. Also, graphene nanoplatelets can improve the interfacial properties of FMLs [23]. Zamani et al. [24] studied the elastic properties and interfacial toughness of carbon fiber metal laminates under interfacial normal and shear stress. Their results revealed that the interfacial fracture toughness of the CFML increases by 0.5 wt.% of nanoclay Cloisite 20A. In addition, improving the mechanical properties of epoxy-clay nanocomposites such as tensile strength, Young's modulus, and fracture

This is the accepted manuscript (postprint) of the following article:
Bahari-Sambran, F., Meuchelboeck, J., Kazemi-Khasragh, E., Eslami-Farsani, R., & Chirani, S. A. (2019). The effect of surface modified nanoclay on the interfacial and mechanical properties of basalt fiber metal laminates. *Thin-Walled Structures*, *144*, 106343.
https://doi.org/10.1016/j.tws.2019.106343

toughness by incorporation of nanoclay in the epoxy matrix has been reported [25, 26]. However, the mechanical properties of epoxy-clay nanocomposites are dependent on the quality of the nanoclay dispersion in the matrix, type of nanocomposite configuration i. e. exfoliation/intercalation and interfacial interactions [27]. Montmorillonite is the popular kind of clay, which is formed of three crystal layers consist of one internal octahedral layer sandwiched between two tetrahedral silicate layers. Montmorillonite is a hydrophilic material which is incompatible with epoxy [28, 29]. Accordingly, to achieve the adequate mechanical properties, the modification of nanoclay with a functional agent consisting of one organo-philic function and one hydrophilic function is necessary. Due to their reaction with the hydroxyl groups of clay layers, silane compounds can be used as a proper agent for functionalization of clay. Functionalization of the inorganic fillers by silane leads to improving the dispersion of them in the polymeric matrix and so, increasing the mechanical properties of epoxy matrix composites [28, 30].

The effect of glass powder addition on edgewise and flatwise Charpy test response of basalt fiber reinforced epoxy and basalt fiber metal laminates (BFML) was investigated by Eslami-Farsani et al. [31]. In another study, Ferrante et al. [32] performed an experimental research on the mechanical behavior of three different FMLs manufactured with Basalt fibers, aluminum, and epoxy resin. Their findings showed the positive effect of basalt fibers on improving the mechanical behavior of FMLs, compared to the glass fibers. Bahari-Sambran et al. [33] investigated the effect of various weight percentages of modified/unmodified nanoclay on the flexural behavior of laminated aluminum epoxy/basalt fibers composites. Their results show the best optimized flexural strength and impact behavior in 3 wt.% of nanoclay.

To the best of our knowledge, the mechanical behavior of BFMLs containing montmorillonite nanoclay focusing on interfacial properties of components has not been studied. Therefore, in this study, with the aim of improving the mechanical properties of BFMLs the effect of adding modified nanoclay on the Charpy and ILSS properties of aluminum 2024-T3-epoxy/basalt fibers composite is investigated. Furthermore, in this study, the FMLs with different fiber orientation were chosen in order to investigate the effect of nanoclay on the fiber direction of FMLs.

2. Experiment

2.1. Materials

In the production procedure of the composite samples, 2024-T3 aluminum sheets having a thickness of 0.5 mm were utilized. The Epon 828 epoxy resin with a polyamine hardener (from Mokarrar Engineering Materials Co.) was used as the matrix. Furthermore, the nanoclay (Montmorillonite k10

This is the accepted manuscript (postprint) of the following article:
Bahari-Sambran, F., Meuchelboeck, J., Kazemi-Khasragh, E., Eslami-Farsani, R., & Chirani, S. A. (2019). The effect of surface modified nanoclay on the interfacial and mechanical properties of basalt fiber metal laminates. *Thin-Walled Structures*, *144*, 106343.
https://doi.org/10.1016/j.tws.2019.106343

from Sigma-Aldrich) and woven basalt fibers (from Basaltex) were utilized as the reinforcements. Finally, to achieve an adequate dispersion of clay nanoparticles in the epoxy matrix, the organo-silane tri-glycidoxy propyl trimethoxysilane (3-GPTS) coupling agent (from Merck) was used. The properties of the materials used in this study are given in Table 1.

Table 1. The properties of materials used to fabrication of BFMLs

Material	**Property (unit)**	**Magnitude**
KER 828 epoxy resin	Density (g/cm^3)	1.16
	Dynamic viscosity, ambient temperature (Pa.S)	12-14
	Boiling point (°C)	200
	Flash point (°C)	200
Basalt fabrics	Weave type	Atlas
	Thickness (mm)	0.19
	Areal density (g/m^2)	350
	Yarn density (ends/cm)	
	Warp	15.0
	Weft	7.5
	Breaking load (N/25mm)	
	Warp	3800
	Weft	1900
	Fiber diameter (µm)	12
Nanoclay	Thickness (nm)	1
	Morphology	Powder
	)m^2/g(Surface covering	250

2.2. The surface treatment of aluminum sheets

The FPL-etching method was conducted on aluminum sheets in order to obtain a proper adhesion between the aluminum sheets and the epoxy resin. In this method, the FPL-etching solution was prepared with the chemical composition of 33.7 g/l sodium dichromate ($Na_2Cr_2O_7$) and 374.5 g/l sulfuric acid. As a first step, the aluminum sheets were cleaned by acetone and immersed in 0.2% NaOH solution for 2 minutes. Then, the aluminum sheets were etched in FPL solution for 30 min at 60 °C. Finally, the aluminum sheets were immersed in distilled water for 5 min and were completely dried in an oven for one hour at 50 °C [34, 35]. Fig. 1 shows the surface morphology of the aluminum sheets before and after surface treatment. As can be seen, a uniform roughness is created on the aluminum surface after the FPL-etching.

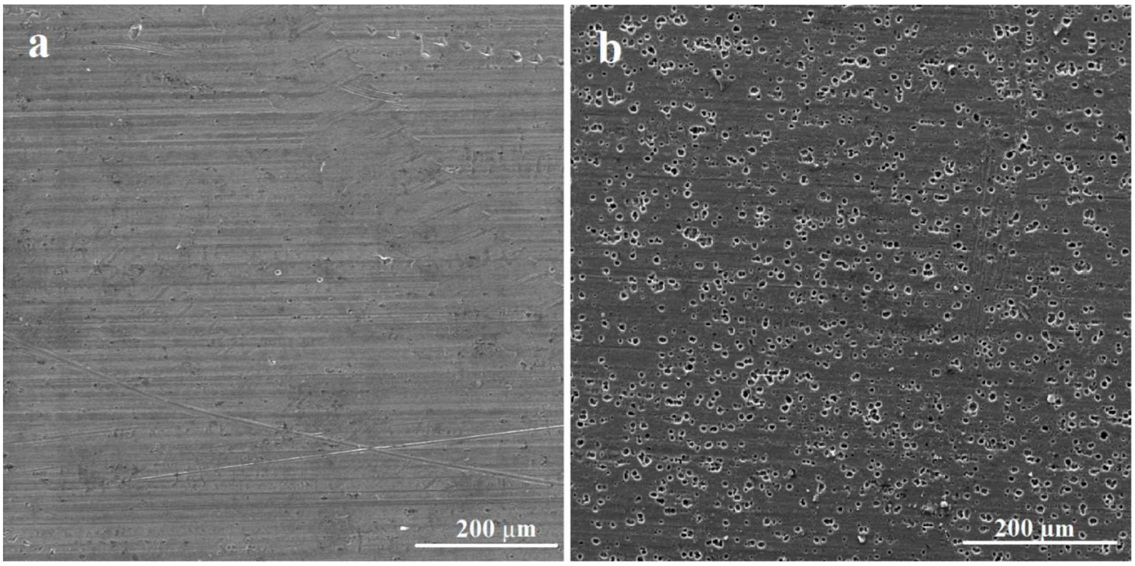

Fig. 1. Surface morphology of the aluminum sheet (a) before surface treatment, (b) after surface treatment.

2.3. Fabrication of BFML samples

The fabrication of BFMLs was conducted by the hand lay-up method. As the first step, the surface-modified nanoclays (the details of surface modification of nanoclay can be observed in Ref. [33]) were added to the epoxy resin with different weight percentages (1, 3, and 5 wt.%) and mixed by a mechanical mixer for 20 min and at 2000 rpm. In addition, to obtain an adequate distribution and dispersion of the surface- modified nanoclay in the matrix and also breaking the agglomerated nanoclay into smaller ones, the mixtures were subjected to the ultrasonic waves for 90 min by means of a homogenizer probe (from Fapen Co.). Afterward, the hardener agent was added to the mixtures. To fabricate the composite samples, four layers of woven basalt fibers in a specific direction and an equal weight ratio of epoxy resin were used. Each layer of woven basalt fibers and the surface of aluminum were separately impregnated with epoxy resin. After the material was laid down, a spiral

This is the accepted manuscript (postprint) of the following article:
Bahari-Sambran, F., Meuchelboeck, J., Kazemi-Khasragh, E., Eslami-Farsani, R., & Chirani, S. A. (2019). The effect of surface modified nanoclay on the interfacial and mechanical properties of basalt fiber metal laminates. *Thin-Walled Structures*, *144*, 106343.
https://doi.org/10.1016/j.tws.2019.106343

roller was used to spread the resin homogeneously throughout the fibers and remove any voids in the fiber structure. The process was repeated until the required configuration was built up. For the sake of comparison, the samples without nanoclay (control sample) were fabricated in the same manner. For the sake of applying uniform pressure to FML plates a flat fixture with the dimension of 20×20 cm^2 was used. The samples were pressed for 1 day at 5 Bar and room temperature to cure completely. Finally, the prepared FML plates were cut by Abrasive water jet cutting technique in two different directions to study how the orientation of the fibers affects the mechanical properties. So longitudinal and transversal samples, with $[0°]_4$ and $[90˚]_4$ direction of warp yarn obtained from the fabricated plates. The shapes of samples are schematically exhibited in Fig. 2.

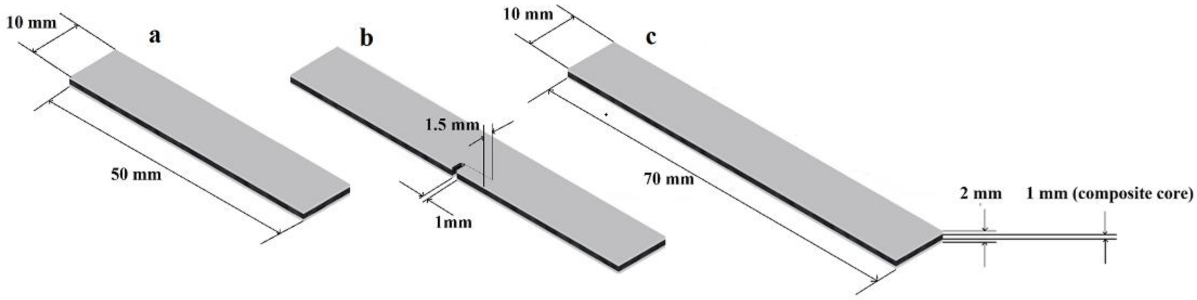

Fig. 2. The schematic illustration of FML samples fabricated for (a) ILSS test, (b) edgewise Charpy test, (c) flatwise Charpy test.

2.4. Charpy test

The Charpy tests were carried out on both longitudinal and transversal samples, $[0°]_4$ and $[90˚]_4$ respectively. Both edgewise and flatwise FML samples with the dimension of 70×10×2 mm^3 (Fig. 2) were tested. As it has been exhibited in Fig. 2b, the U-notch with the dimension of 1 and 1.5 mm, width and depth, respectively created at the middle of the edgewise sample. The test was performed by means of digital pendulum Charpy indicator (Santam SIT 200B) and stored energy of 200 J. The recommendations of ISO 179-1 are followed for the Charpy test conditions in this research. However, because of the lower thickness of samples and span length the length of the samples is considered 70 mm. In this test, the dissipated energy due to the air resistance and bearing friction was neglected. For all samples, the tests were repeated five times, at least. The schematic images of the edgewise and flatwise Charpy test are illustrated in Fig. 3.

This is the accepted manuscript (postprint) of the following article:
Bahari-Sambran, F., Meuchelboeck, J., Kazemi-Khasragh, E., Eslami-Farsani, R., & Chirani, S. A. (2019). The effect of surface modified nanoclay on the interfacial and mechanical properties of basalt fiber metal laminates. *Thin-Walled Structures*, *144*, 106343.
https://doi.org/10.1016/j.tws.2019.106343

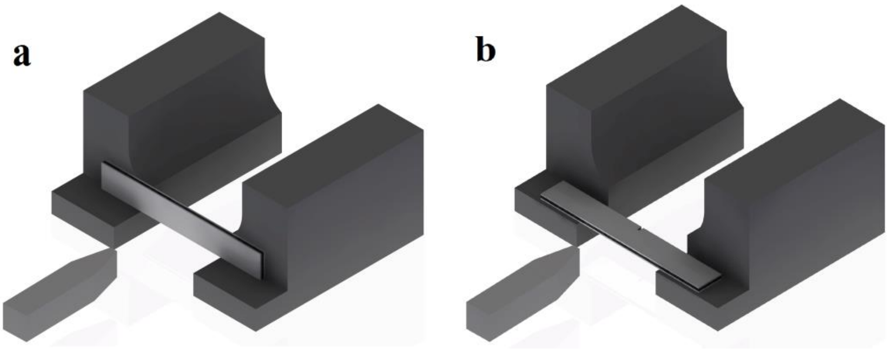

Fig. 3. The schematic of the FML sample under Charpy test (a) flatwise Charpy test, (b) edgewise Charpy test.

2.5. Interlaminar shear strength (ILSS)

Characterizing the ILSS of FML samples was performed by short beam shear (SBS) method on both longitudinal and transversal samples. The rectangular samples with the dimension of 50×10×2 mm^3 (Fig. 2c) were tested in three-point bending, at least five times. For this test, the 10-ton Koopa test machine was used and according to literature, the span-to-thickness ratio of the sample was selected 1/t=10 [3, 11]. In addition, loading was carried out with a constant nose movement with a rate of 1 mm/min and the bending force-displacement diagram was derived by the machine. Table 2 represents the experimental conditions of the Charpy and ILSS tests. The SBS test of FML sample is depicted in Fig. 4. The failure load was utilized to determine the interlaminar shear strength of the FML samples and the short beam strength of the samples was calculated by the equation (1):

$$\tau = \frac{3P_m}{4wt} \tag{1}$$

Where P_m is the maximum load in short-beam three-point bending test and t and w are the thickness and width of the sample, respectively [10, 36].

This is the accepted manuscript (postprint) of the following article:
Bahari-Sambran, F., Meuchelboeck, J., Kazemi-Khasragh, E., Eslami-Farsani, R., & Chirani, S. A. (2019). The effect of surface modified nanoclay on the interfacial and mechanical properties of basalt fiber metal laminates. *Thin-Walled Structures*, *144*, 106343.
https://doi.org/10.1016/j.tws.2019.106343

Table 2. The experimental conditions of the applied tests

Test	Parameter	Values
Edgewise Charpy	Dimension (length × width × thick) (mm)	70×10×2
	Stored energy (J)	200
	U-notch dimension (depth × width) (mm)	1.5×1
	Flash point (°C)	200
Flatwise Charpy	Dimension (length × width × thick) (mm)	70×10×2
	Stored energy (J)	200
ILSS	Nose movement rate (mm/min)	1
	Dimension (length × width × thick) (mm)	50×10×2
	Span-to-depth ratio (L/h)	1/10
	Radius of loading nose (mm)	3
	Radius of supports (mm)	3

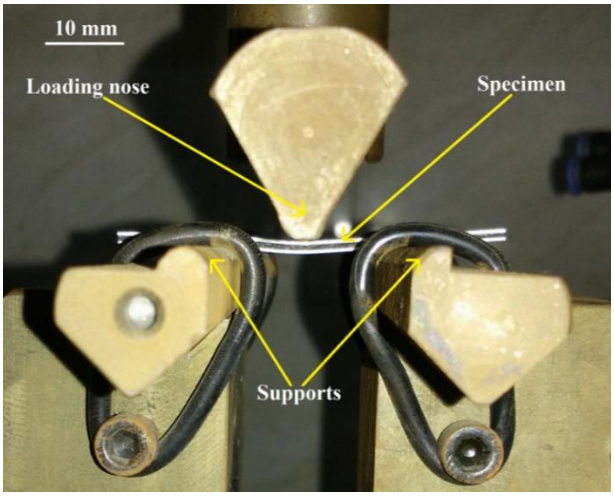

Fig. 4. Short beam shear test.

2.6. Structural and microscopic analysis

The structural changes of nanoclay and its composites were examined by X-ray diffraction (XRD, Siemens D500, Germany) with Cu radiation (λ=0.154 nm). Strengthening mechanisms of nanoclay and debonding surface between epoxy/basalt fibers and epoxy/aluminum was studied by field emission scanning electron microscopy (FESEM) model MIRA3TESCAN-XMU and scanning electron microscopy (SEM) model VEGA\\TESCAN-XMU. In addition, the fracture and delamination occurred in FML samples were analyzed by means of optical microscopy (OP).

This is the accepted manuscript (postprint) of the following article:
Bahari-Sambran, F., Meuchelboeck, J., Kazemi-Khasragh, E., Eslami-Farsani, R., & Chirani, S. A. (2019). The effect of surface modified nanoclay on the interfacial and mechanical properties of basalt fiber metal laminates. *Thin-Walled Structures*, *144*, 106343.
https://doi.org/10.1016/j.tws.2019.106343

3. Results and discussion

3.1. Microstructure of the composite

The structures of nanoclay with different weight percents in the nanocomposites were detected by XRD analysis, as exhibited in Fig. 5. Pure epoxy represents a broad peak at 17.9°, which is attributed to the amorphous nature of the polymer [37]. A sharp peak at 8.5° in pristine nanoclay is attributed to the 001 reflection. For the nanocomposites containing 1, 3, and 5 wt.% nanoclay the 001 reflection of nanoclay is shifted to 4.6°, 5.1°, and 6.7°, respectively which demonstrates that the d001 spacing of nanoclay has expanded and intercalated state is reached [38]. This indicates that hardener or resin has inserted into the galleries of the clay [39]. In addition, at lower clay loadings in epoxy, the peaks shifted to lower 2θ or larger d-spacing. The peak shift indicates that the agglomeration has occurred in higher loading of nanoclay.

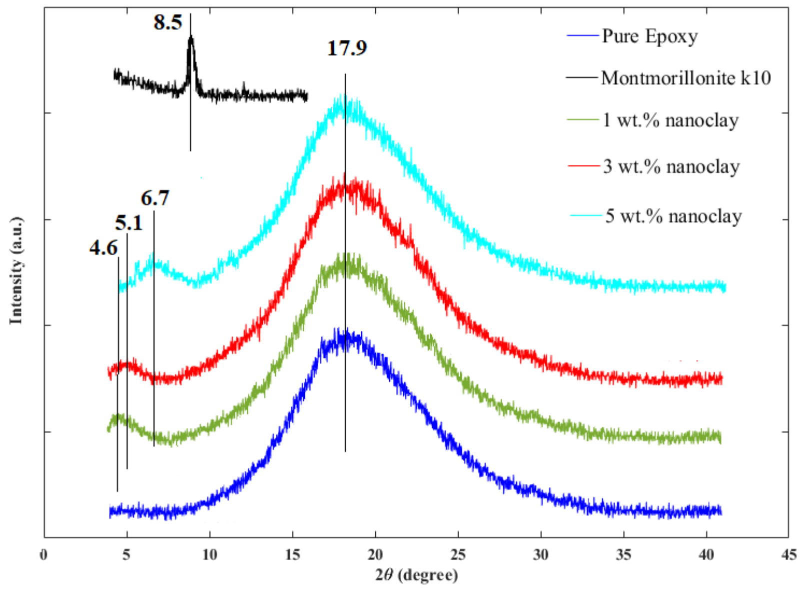

Fig. 5. XRD patterns of composites containing various weight percentages of nanoclay.

3.2. Charpy test

The average of absorbed energy values obtained by Charpy tests are given in Table 3. By analyzing the absorbed energy values, it is possible to compare the mechanical properties of both longitudinal $[0°]_4$ and transversal $[90°]_4$ BFMLs.

This is the accepted manuscript (postprint) of the following article:
Bahari-Sambran, F., Meuchelboeck, J., Kazemi-Khasragh, E., Eslami-Farsani, R., & Chirani, S. A. (2019). The effect of surface modified nanoclay on the interfacial and mechanical properties of basalt fiber metal laminates. *Thin-Walled Structures*, *144*, 106343.
https://doi.org/10.1016/j.tws.2019.106343

Table 3. The obtained results of Charpy tests

Nanoclay loading (wt.%)	Absorbed energy by flatwise $[0°]_4$ sample (J)	Absorbed energy by flatwise $[90°]_4$ sample (J)	Absorbed energy by edgewise $[0°]_4$ sample (J)	Absorbed energy by edgewise $[90°]_4$ Sample (J)
0	10.52±0.57	3.97±0.13	4.78±0.28	2.44±0.08
1	11.28±0.66	4.08±0.13	4.98±0. 31	2.47±0.10
3	11.94 ±0.55	4.20±0.12	5.21±0.34	2.51±0.09
5	10.82±0.64	4.02±0.14	4.87±0.28	2.45±0.11

As it is given in Table 1, the yarn density of basalt fibers is 15 and 7.5 (ends/cm) in the longitudinal and transversal direction, respectively. The obtained results of adding various weight percentages of nanoclay on the energy absorption of BFML samples with both longitudinal and transversal directions have been presented in Fig. 6. As it can be observed, in the case of BFML without nanoclay, the absorbed energy value of the longitudinal sample is about 165% higher than that of the transversal sample, in flatwise test. Similar to the edgewise test, the longitudinal sample indicates a 96% increase inthe absorbed energy value compared to the transversal sample. This comparison of the longitudinal and transversal samples expresses the importance of fiber orientation and its significant influence on the mechanical properties of FMLs. Concerning the effect of nanoclay on energy absorption, for all cases, there is an upward trend up to 3 wt.% then it is transformed into a downward drift. The absorbed energy of the samples containing 3 wt.% nanoclay in cases of flatwise $[0°]_4$, flatwise $[90°]_4$, edgewise $[0°]_4$ and edgewise $[90°]_4$ is elevated 13.5, 5.8, 9 and 2.8 percent respectively, compared to the similar samples without nanoclay. These data indicate a more dominant effect of nanoclay on longitudinal samples as compared to transversal samples. Therefore, it can be concluded that the influence of nanoclay on improving the interface characteristics and load transfer mechanism from the matrix to the fibers is significant [40]. Moreover, the addition of nanoclay results in entanglement between the polymer chains and nanoclay layers which could improve the strength and absorbed energy values.

According to Fig. 6, the absorbed energy of all samples containing 5 wt.% nanoclay has reduced in comparison with the similar samples containing 3 wt.% nanoclay. This can be attributed to the improper distribution and agglomeration of nanoclay in higher concentrations. Due to the presence of nanoclay agglomerations, the interface of fiber–matrix is prone to failure. In addition, the created

This is the accepted manuscript (postprint) of the following article:
Bahari-Sambran, F., Meuchelboeck, J., Kazemi-Khasragh, E., Eslami-Farsani, R., & Chirani, S. A. (2019). The effect of surface modified nanoclay on the interfacial and mechanical properties of basalt fiber metal laminates. *Thin-Walled Structures*, *144*, 106343.
https://doi.org/10.1016/j.tws.2019.106343

agglomerations would lead to the formation of stress concentration points. Furthermore, with increasing the concentrations of nanoclay particles in the epoxy resin, the viscosity of resin increases. In fact, higher viscosity of the resin cause to imprison more air bubbles in the mixture during the mixing process which leads to defects and consequently weakens the composite properties [33, 41].

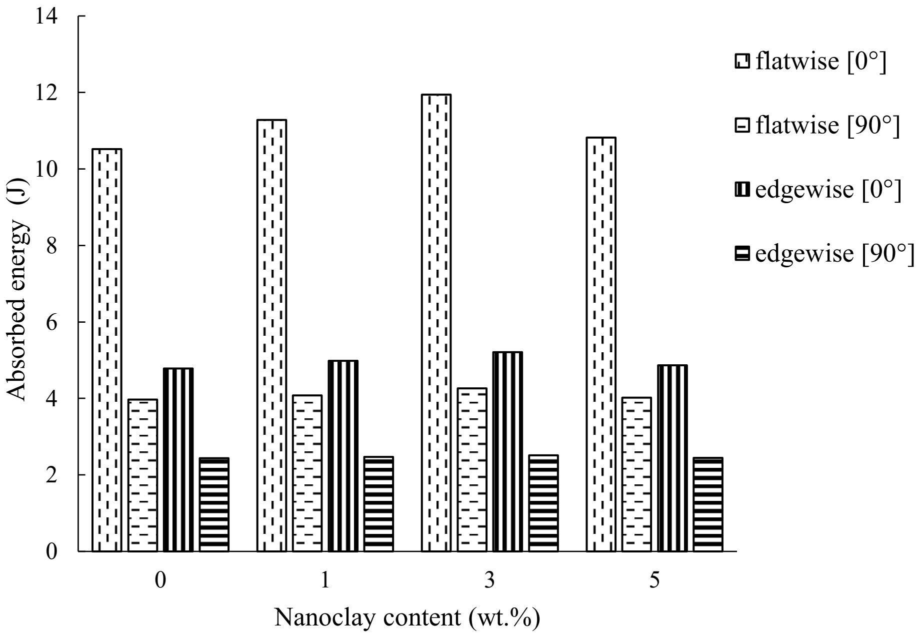

Fig. 6. Absorbed energy by BFML samples with different fiber orientation and nanoclay content under edgewise and flatwise Charpy test.

3.3. Investigation of the fracture nature

In fact, the main energy absorption mechanisms include the fracture in any layer of the FML, fiber breakage, delamination, plastic deformation of the aluminum layer, fiber pull-out and debonding in the composite and metallic sections. These energy absorption mechanisms depend on the mechanical properties of the FML, interaction between the matrix and fibers as well as the matrix with the metal sheet and its combination [42]. Fig. 7 shows the failure modes of four BFML samples with various fiber orientations and Charpy test type. Plastic deformation of the aluminum layer and matrix cracking have occurred for all specimens. In the case of the longitudinal sample (Fig. 7a), the aluminum rupture, delamination, debonding in the composite and metallic sections and fiber breakage are the main contributing energy absorption mechanisms. Therefore, the absorbed energy of this sample is relatively high. However, the debonding at polymer/aluminum interface is the only absorption mechanism for the transversal sample (Fig. 7c) which is the main reason for lesser absorbed energy value of it, compared to the longitudinal sample. Moreover, the sharp bending angle of the sample at the strike location of the transversal sample (Fig. 7c) is because of the low load resistance and matrix failure. However, the [0º] direction of fibers in the longitudinal sample increases the strength of FML. Concerning the edgewise Charpy test samples (Figs. 7b and 7d), the longitudinal sample (Fig. 7b) indicates aluminum rupture, debonding and fiber breakage which have resulted in high energy absorption. However, the aluminum rupture and fiber breakage can be seen in transversal one. Hence, a larger damage area due to contributing different energy dissipation mechanisms can result in a higher amount of total energy absorption.

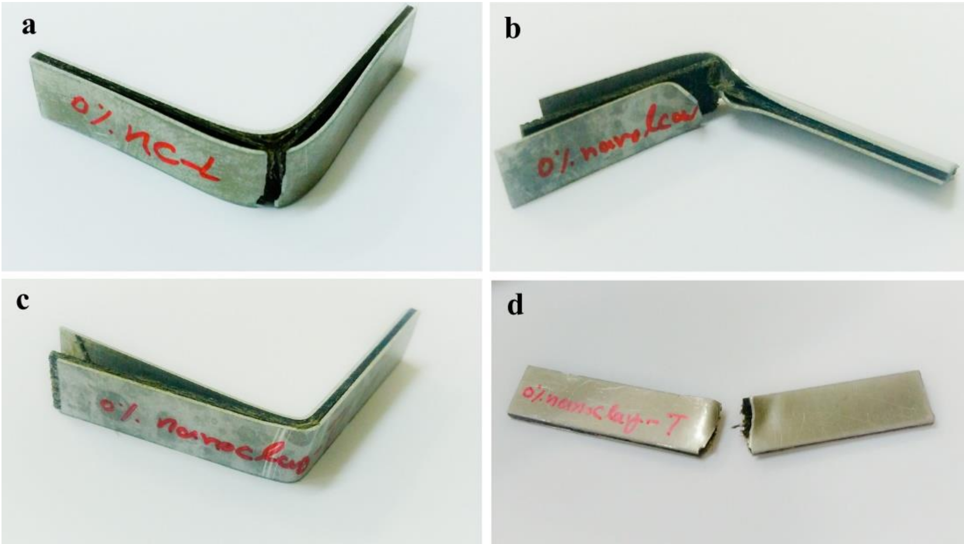

Fig. 7. (a) longitudinal specimen after flatwise Charpy test, (b) longitudinal specimen after edgewise Charpy test, (c) transversal specimen after flatwise Charpy test, (d) transversal specimen after edgewise Charpy test.

Fig. 8 displays the damage area and bending angle of the tested specimens containing various percentages of modified nanoclay. In all the specimens rupture and plastic deformation of aluminum, fiber breakage, delamination, and the fracture in the matrix could be easily seen. As it is indicated, the bending angle is decreased by increasing the nanoclay up to 3 wt.%. Reducing the bending angle with the addition of nanoclay could be due to reinforcing the composite core, fracture strain rise, increase in bending strength and decrease in fractured fibers [33]. Increasing the bending angle in the sample containing 5 wt.% modified nanoclay (Fig. 8d) as compared with 3 wt.% one (Fig. 8c) can be related to the agglomeration of the modified nanoclay in the epoxy matrix and consequently, weakening the bending strength. Moreover, the fiber breakage and delamination also happened more remarkably in the sample containing 5 wt.% modified nanoclay which is a result of the agglomeration of nanoclay.

This is the accepted manuscript (postprint) of the following article:
Bahari-Sambran, F., Meuchelboeck, J., Kazemi-Khasragh, E., Eslami-Farsani, R., & Chirani, S. A. (2019). The effect of surface modified nanoclay on the interfacial and mechanical properties of basalt fiber metal laminates. *Thin-Walled Structures*, *144*, 106343.
https://doi.org/10.1016/j.tws.2019.106343

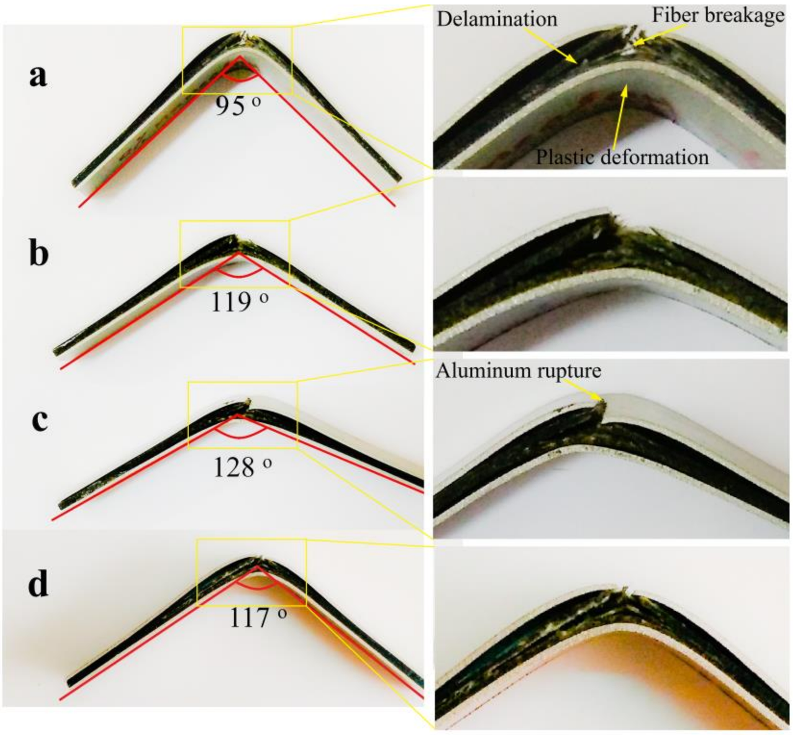

Fig. 8. Bending angle of the longitudinal FML samples after flatwise Charpy test (a) without nanoclay, (b) with the 1 wt.% modified nanoclay, (c) with the 3 wt.% modified nanoclay, (d) with the 5 wt.% modified nanoclay.

3.4. Characterization of the ILSS by short beam shear test

Generally, when the transverse shear stress exceeds the interfacial shear strength, an interfacial debonding occurs. Figs. 9a and 9b show the short beam shear test results of longitudinal and transversal BFML samples. As it can be observed, for both types of samples, the failure occurs at the sharp decline of the load which demonstrates the occurrence of debonding in laminates [3, 36]. Regarding the Figs. 9a and 9b, it can be said that the addition of different weight percentages of nanoclay leads to decrease of the failure loads. Fig. 10 shows the load-deflection curves of different BFML samples. As shown, the interlaminar failure behavior is affected by the fibers direction. Comparison of the failure loads of samples reveals that the sample with longitudinal fiber ([0°]) configuration shows higher shear strength. The longitudinal fibers in FMLs contribute to supporting the laminates and increasing the bending stiffness. However, the higher deflection and lower failure load of the sample with transversal fiber direction ([90°]) with compared to longitudinal sample ([0°]) is due to decrease in bending stiffness and supporting of the laminates by fibers. Regarding the area under the load-deflection curves, the absorbed energy of longitudinal and transversal FML samples are 911 N.mm and 870 N.mm, respectively. As it is clear, there is no significant difference between

This is the accepted manuscript (postprint) of the following article:
Bahari-Sambran, F., Meuchelboeck, J., Kazemi-Khasragh, E., Eslami-Farsani, R., & Chirani, S. A. (2019). The effect of surface modified nanoclay on the interfacial and mechanical properties of basalt fiber metal laminates. *Thin-Walled Structures*, *144*, 106343.
https://doi.org/10.1016/j.tws.2019.106343

the absorbed energies by two types of samples. It means that the debonding in the interface of composite core and aluminum layer plays an important role in energy absorption.

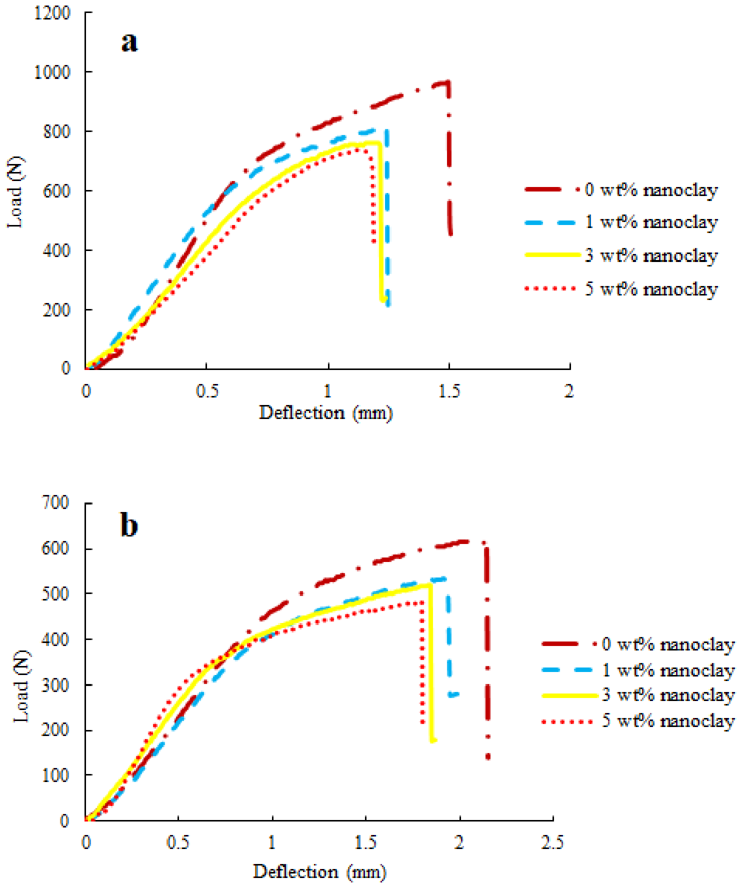

Fig. 9. Load-deflection curves of BFMLs containing different weight percentages of nanoclay (a) longitudinal BFML sample, (b) transversal BFML sample.

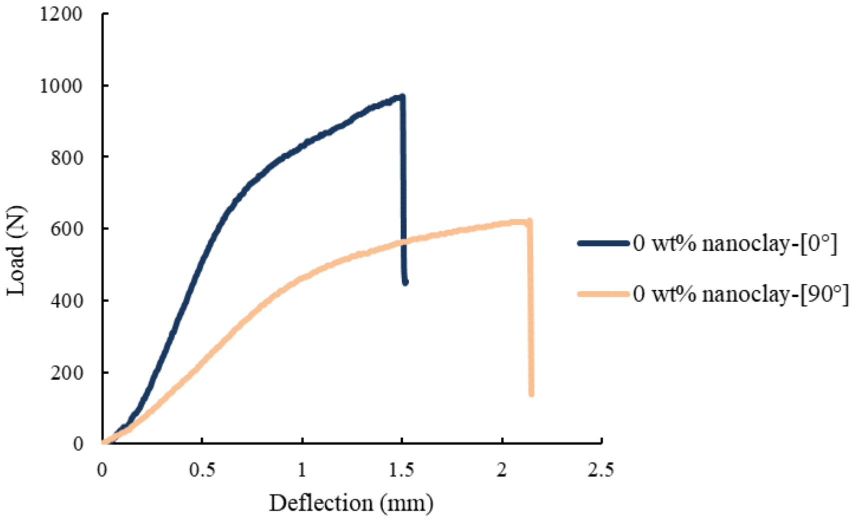

Fig. 10. Comparison of load-deflection curves of FMLs with different fiber direction.

The variation of ILSS values of BFMLs as a function of the nanoclay particles concentrations are presented in Fig. 11. As can be seen, in case of the longitudinal FML, ILSS of the samples is declined by 15.7, 21.2 and 23.8 percent with the increase of 1, 3 and 5 wt.% of the modified nanoclay, respectively, as compared to the FMLs without nanoclay. Moreover, the results of the transversal FMLs show that 1, 3 and 5 wt.% of the modified nanoclay reduces the ILSS by 13.9, 20.1 and 23.5 percent, respectively, with respect to the FMLs without nanoclay. It seems that the reducing effect of nanoclay particles on the ILSS values is affected by the interfacial properties of the polymeric matrix and the aluminum layer which is a weaker part of the FML. As mentioned earlier, the addition of the nanoclay leads to increase in the viscosity of the epoxy resin. The effect of increasing the polymer's viscosity on the mechanical behavior of FMLs can be characterized by two aspects. First, with increasing the polymer's viscosity the number of trapped bubbles increases and so, the extracting of these bubbles becomes difficult. The presence of trapped babbles at the polymer-aluminum interface can cause to the weakening of the adhesion and so, mechanical properties of the FML. Second, increasing the polymer's viscosity caused by the addition of nanoclay particles can reduce the liquidity and wettability characteristics of resin on the aluminum surface and consequently, reducing the adhesion. In addition, the agglomerated particles could reduce the quality of adhesion by preventing the resin penetration in the micro-scale cavities and porous structure created by FPL-etching technique. Reduction in ILSS values can also be due to the fact that the nanoparticles do not adhere to the aluminum and act as stress-raisers. With a comparison between the results of Charpy and ILSS tests, this question can be considered why the poor interfacial aluminum/composite

This is the accepted manuscript (postprint) of the following article:
Bahari-Sambran, F., Meuchelboeck, J., Kazemi-Khasragh, E., Eslami-Farsani, R., & Chirani, S. A. (2019). The effect of surface modified nanoclay on the interfacial and mechanical properties of basalt fiber metal laminates. *Thin-Walled Structures*, *144*, 106343.
https://doi.org/10.1016/j.tws.2019.106343

adhesion does not seem to play a role in the Charpy tests. In fact, the value of the span-to-thickness ratio changes the failure mode of FML. Therefore, in the Charpy test, the other failure mechanisms are dominated before a shear dominant failure. In other words, the distribution of stress in Charpy and ILSS test is completely different. The Charpy impact test is a dynamic three-point bending. Fig. 12 displays the conditions of the Charpy test on the fiber reinforced composite with varying step time [43]. It shows that the concentration of stress is at the strike location of the sample which may result in, fiber breakage, delamination, plastic deformation of the aluminum layer, fiber pull-out, and debonding in the composite and metallic sections. It is proved that the nanoclay improves the mechanical properties of basalt fiber reinforced composites by increasing the stress level required for fiber failure and affecting the load transfer mechanism from the matrix to the fibers [44]. Hence, it can be deduced that the mentioned mechanisms mainly leads to improve impact properties of BFML. However, in the case of the ILSS test, basalt fibers do not contribute to energy dissipation and the failure mechanism is debonding in the composite and metallic sections.

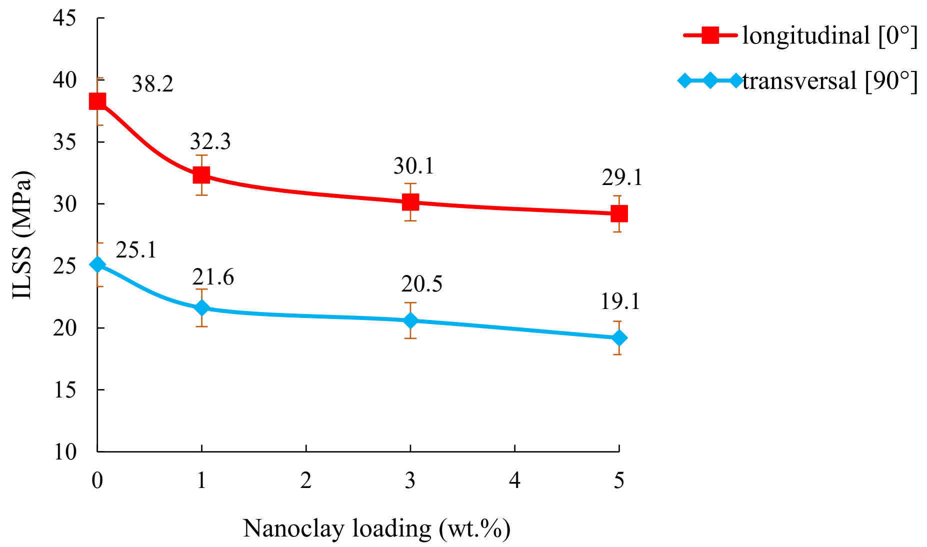

Fig. 11. The ILSS of BFML containing various weight percentages of surface-modified nanoclay.

This is the accepted manuscript (postprint) of the following article:
Bahari-Sambran, F., Meuchelboeck, J., Kazemi-Khasragh, E., Eslami-Farsani, R., & Chirani, S. A. (2019). The effect of surface modified nanoclay on the interfacial and mechanical properties of basalt fiber metal laminates. *Thin-Walled Structures*, *144*, 106343.
https://doi.org/10.1016/j.tws.2019.106343

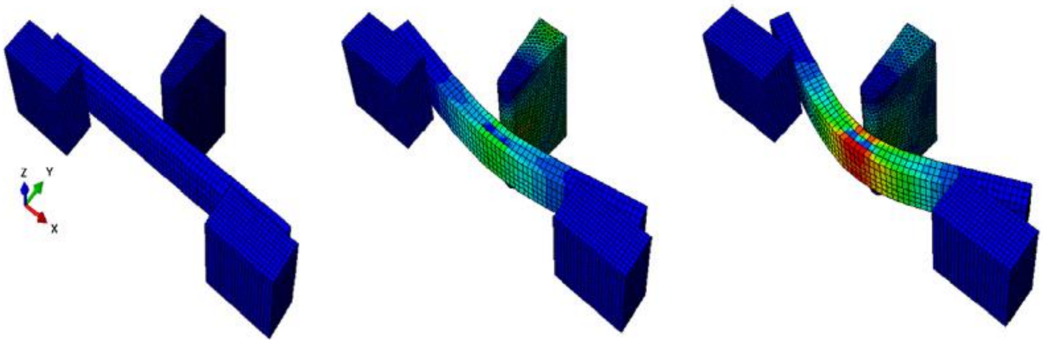

Fig. 12. Simulation condition of Charpy impact test with different step time [43].

3.5. Shear failure characteristics of BFML

Failure modes of two BFML samples with different fiber orientation are presented in Fig. 13. It is obvious that the failure deflection for the transversal sample (Fig. 13b) is higher than that of the longitudinal sample (Fig. 13a). This observation illustrates that the fiber direction affected the interlaminar failure behavior, and the higher deflection can be attributed to the lack of supporting the laminates by fibers and low bending stiffness. On the other hand, according to the ILSS test results, the longitudinal sample indicates a higher shear strength and failure load with a lower deflection. As it was mentioned above, there is no significant difference between the absorbed energies by two types of samples. In the case of the longitudinal specimen, aluminum-composite debonding is the main energy dissipation mechanism which higher density of fibers along the length direction of the specimen dominates in the load and energy absorption capacity of the laminates [11, 45]. In transversal specimen, the local flexural failure such as buckling and fiber breakage takes part in energy dissipation (Fig. 13b). However, according to the load-deflection curve of this specimen, the main energy dissipation mechanism is the aluminum-composite debonding. As it can be observed in Fig. 13b, buckling has occurred and a group of fibers has fractured at the upper side of the transversal sample. With increasing the stress concentration near the loading nose, the large deflection induces higher compressive stress in the interlayer, and cause buckling failure. It was expected that the debonding occurred in the middle of the span. According to the theories of the beam, the distribution of the shear stress in the thickness direction is parabolic [11]. For both samples, debonding occurred at the aluminum-composite core interface. This confirms that the aluminum-composite core interface is weaker than epoxy-basalt fibers interface.

This is the accepted manuscript (postprint) of the following article:
Bahari-Sambran, F., Meuchelboeck, J., Kazemi-Khasragh, E., Eslami-Farsani, R., & Chirani, S. A. (2019). The effect of surface modified nanoclay on the interfacial and mechanical properties of basalt fiber metal laminates. *Thin-Walled Structures*, *144*, 106343.
https://doi.org/10.1016/j.tws.2019.106343

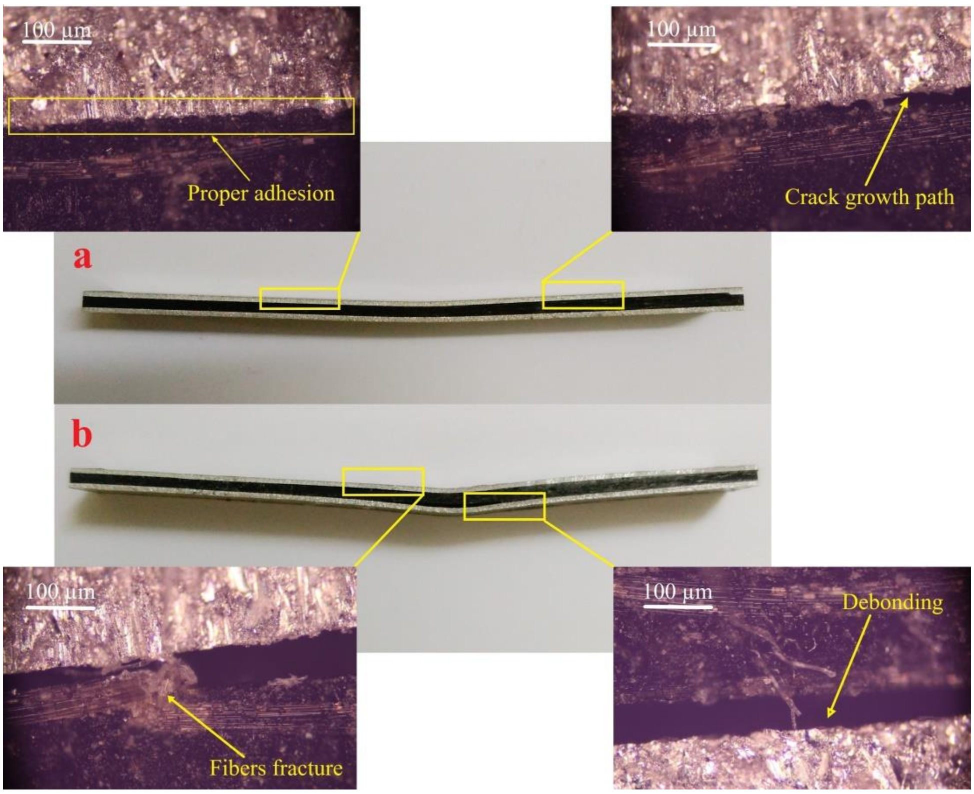

Fig. 13. Failure modes after short-beam shear test, (a) longitudinal specimen, (b) transversal specimen.

3.6. Macroscopic and microscopic analysis of the fracture surfaces

Fig. 14 shows the FESEM images of the fracture surface of composite cores after Charpy tests. In the case of the sample without nanoclay (Fig. 14a), the surface of the basalt fibers are very smooth and there is no significant bonding between the epoxy resin and basalt fibers. However, in the samples containing surface modified nanoclay, the epoxy resins partially adhered to the basalt fibers. In the case of 3 wt.% nanoclay sample, this phenomenon is significant. As can be seen in Fig. 14c, the addition of 3 wt.% nanoclay has led to increasing the ductility and toughness of the epoxy matrix, confirming the enhancement of mechanical properties of the BFMLs containing nanoclay. These observations are in good agreement with Withers et al. [40] study. They have also reported that the addition of nanoclay results in ductile like matrix features. Comparison of two fracture surfaces confirms the positive effect of the surface-modified nanoclay on improving the interfacial basalt fibers-epoxy adhesion.

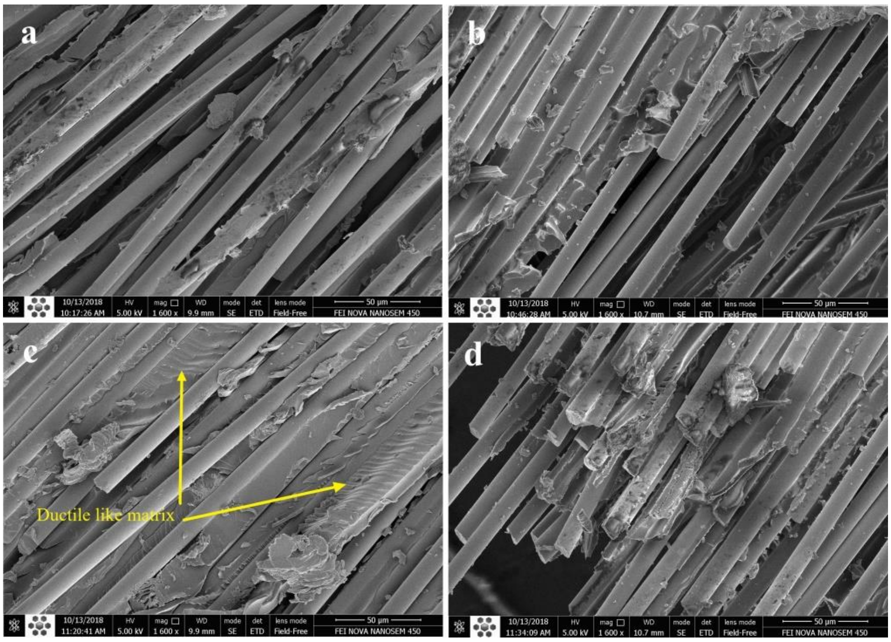

Fig. 14. FESEM photographs of the fracture surfaces of basalt/epoxy composites (a) without nanoclay, (b) with 1 wt.% modified nanoclay, (c) with 3 wt.% modified nanoclay, (d) with 5 wt.% modified nanoclay.

To better understand the effect of nanoclay on the interfacial properties of aluminum-epoxy/basalt fibers, the photographs and FESEM images of debonding surfaces at different magnifications are shown in Figs. 15 and 16. According to Fig. 15, the failure type of all the samples is a combination of cohesive and adhesive. However, with increasing the nanoclay loading the failure occurs more adhesively. Figs. 16b and 16c, exhibit the debonding surface of the sample without nanoclay which has failed adhesively. An adequate infiltration of the epoxy into the porous structures can provide a relatively proper adhesion between the aluminum and epoxy resin. However, in the samples containing 1, 3, and 5 wt.% of nanoclay (Figs. 16d, 16e, 16h, and 16i) inappropriate resin infiltration could be observed. So that the agglomerated nanoclay have prevented the resin infiltration into the porous structures in the sample containing 5 wt.% of nanoclay (Fig. 16i). In Fig.16h, some empty cavities are visible which can be attributed to the effect of nanoclay on the liquidity and wettability characteristics of the epoxy resin. Therefore, it can be concluded that the addition of nanoclay can weaken the interfacial properties and interlaminar shear strength of aluminum/epoxy. Moreover, the agglomerated nanoclay is shown in Fig. 16f which is related to composite core of the sample containing 5 wt.% of nanoclay.

This is the accepted manuscript (postprint) of the following article:
Bahari-Sambran, F., Meuchelboeck, J., Kazemi-Khasragh, E., Eslami-Farsani, R., & Chirani, S. A. (2019). The effect of surface modified nanoclay on the interfacial and mechanical properties of basalt fiber metal laminates. *Thin-Walled Structures*, *144*, 106343.
https://doi.org/10.1016/j.tws.2019.106343

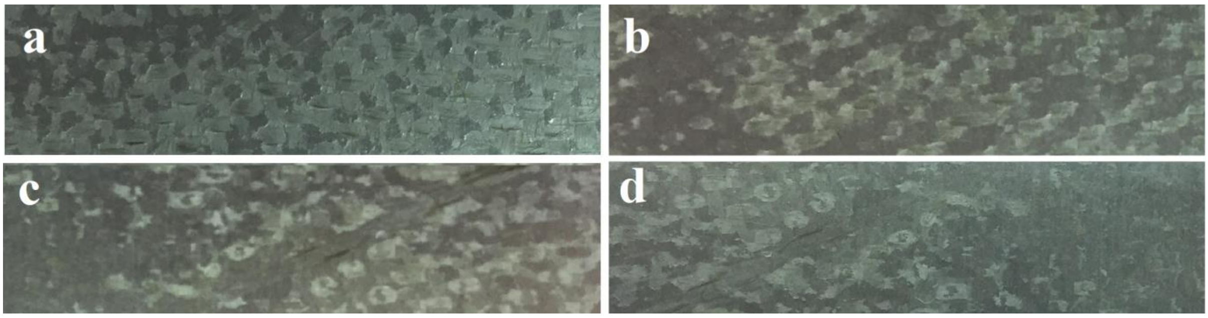

Fig. 15. Debonding surfaces of the specimens (a) without nanoclay, (b) with 1 wt.% modified nanoclay, (c) with 3 wt.% modified nanoclay, (d) with 5 wt.% modified nanoclay.

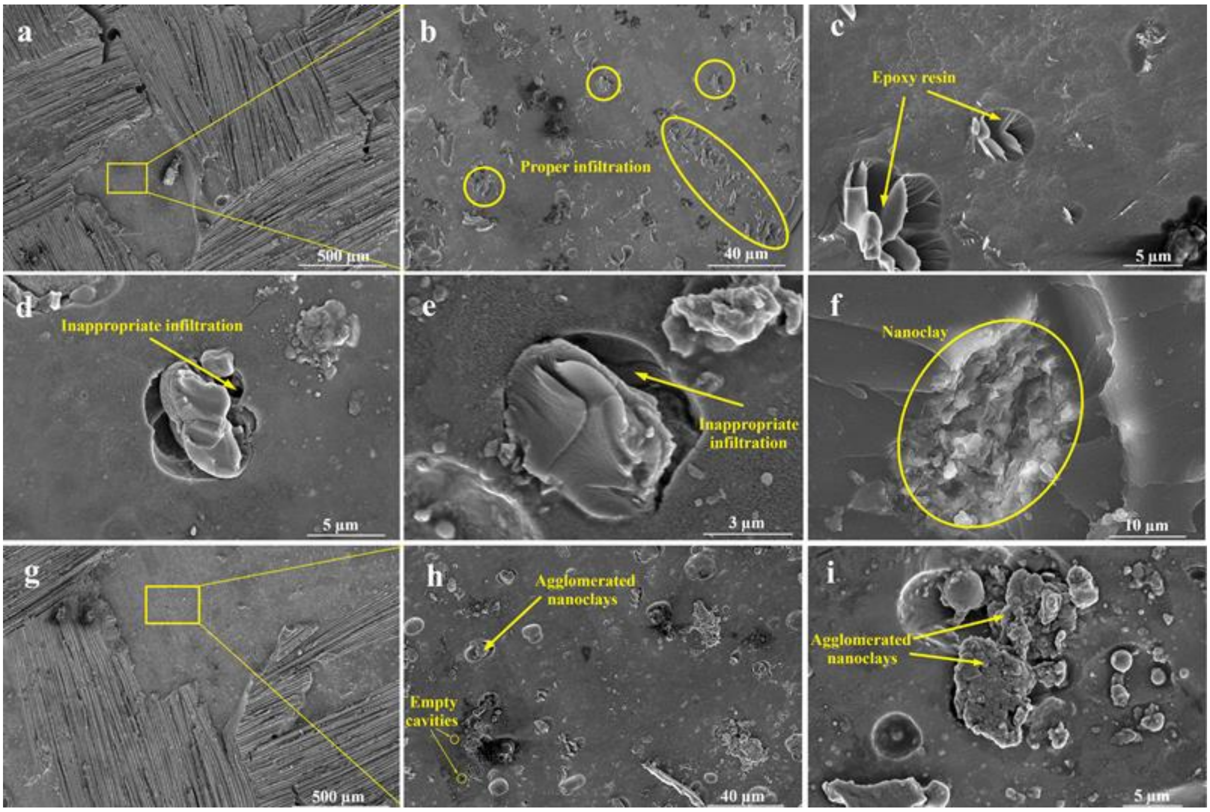

Fig. 16. The FESEM images of debonding surfaces at different magnification (a, b, and c) aluminum surface of the sample without nanoclay, (d) with 1 wt.% of nanoclay, (e) with 3 wt.% nanoclay, (f) composite core with 5 wt.% nanoclay, (g, h, and i) aluminum surface of the samples with 5 wt.% nanoclay.

4. Conclusions

This is the accepted manuscript (postprint) of the following article:
Bahari-Sambran, F., Meuchelboeck, J., Kazemi-Khasragh, E., Eslami-Farsani, R., & Chirani, S. A. (2019). The effect of surface modified nanoclay on the interfacial and mechanical properties of basalt fiber metal laminates. *Thin-Walled Structures*, *144*, 106343.
https://doi.org/10.1016/j.tws.2019.106343

In this study, the effects of adding surface-modified nanoclay (1, 3, and 5 wt.%) on the mechanical behavior of longitudinal and transversal basalt fibers- epoxy/aluminum laminate composites were investigated. The following conclusions were drawn:

1. The addition of surface modified nanoclay increased the energy absorption of both longitudinal and transversal basalt fiber metal laminates under edgewise and flatwise Charpy test. The best energy absorption result was achieved with 3 wt.% nanoclay.
2. The higher impact strength of basalt fiber metal laminate containing nanoclay can be due to the enhancement of the epoxy/basalt fibers interfacial properties and creating some physical entanglement by adding the modified nanoclay.
3. The absorbed energy of all samples containing 5 wt.% modified nanoclay was lower than those of similar samples containing 3 wt.% nanoclay. These findings might come from an improper dispersion and agglomeration of nanoclay at higher concentrations.
4. The interlaminar failure behavior of fiber metal laminates was considerably affected by fiber direction. The longitudinal fibers in fiber metal laminates, contribute in the supporting the laminates and increasing the bending stiffness and strength.
5. The addition of nanoclay decreased the interlaminar shear strength of aluminum/epoxy by preventing the resin infiltration into porous structures.

References

[1] A. Vlot, J.W. Gunnink, Fibre metal laminates: an introduction, Springer Science & Business Media, 2011.

[2] M. Sadighi, R. Alderliesten, R. Benedictus, Impact resistance of fiber-metal laminates: a review, International Journal of Impact Engineering, 49 (2012) 77-90.

[3] S. Zeng, M. Shen, L. Yang, Y. Xue, F. Lu, S. Chen, Self-assembled montmorillonite–carbon nanotube for epoxy composites with superior mechanical and thermal properties, Composites Science and Technology, 162 (2018) 131-139.

[4] M.A. Azghan, R. Eslami-Farsani, The effects of stacking sequence and thermal cycling on the flexural properties of laminate composites of aluminium-epoxy/basalt-glass fibres, Materials Research Express, 5 (2018) 025302.

[5] G.H. Payeganeh, F.A. Ghasemi, K. Malekzadeh, Dynamic response of fiber–metal laminates (FMLs) subjected to low-velocity impact, Thin-Walled Structures, 48 (2010) 62-70.

[6] G.B. Chai, P. Manikandan, Low velocity impact response of fibre-metal laminates–A review, Composite Structures, 107 (2014) 363-381.

[7] R. Alderliesten, Designing for damage tolerance in aerospace: A hybrid material technology, Materials & Design, 66 (2015) 421-428.

[8] T. Sinmazçelik, E. Avcu, M.Ö. Bora, O. Çoban, A review: Fibre metal laminates, background, bonding types and applied test methods, Materials & Design, 32 (2011) 3671-3685.

[9] Y. Lin, Y. Huang, T. Huang, B. Liao, D. Zhang, C. Li, Characterization of progressive damage behaviour and failure mechanisms of carbon fibre reinforced aluminium laminates under three-point bending, Thin-Walled Structures, 135 (2019) 494-506.

[10] H.G. Kotik, J.E.P. Ipiña, Short-beam shear fatigue behavior of fiber metal laminate (Glare), International Journal of Fatigue, 95 (2017) 236-242.

[11] C. Liu, D. Du, H. Li, Y. Hu, Y. Xu, J. Tian, G. Tao, J. Tao, Interlaminar failure behavior of GLARE laminates under short-beam three-point-bending load, Composites Part B: Engineering, 97 (2016) 361-367.

[12] E. Kazemi-Khasragh, F. Bahari-Sambran, M.H. Siadati, R. Eslami-Farsani, High Velocity Impact Response of Basalt Fibers/Epoxy Composites Containing Graphene Nanoplatelets, Fibers and Polymers, 19 (2018) 2388-2393.

[13] J. Sim, C. Park, Characteristics of basalt fiber as a strengthening material for concrete structures, Composites Part B: Engineering, 36 (2005) 504-512.

[14] O. Medvedyev, Y. Tsybulya, Basalt use in hot gas filtration, Filtration & separation, 42 (2005) 34-37.

[15] V. Fiore, T. Scalici, G. Di Bella, A. Valenza, A review on basalt fibre and its composites, Composites Part B: Engineering, 74 (2015) 74-94.

[16] H. Yoder Jr, C.E. Tilley, Origin of basalt magmas: an experimental study of natural and synthetic rock systems, Journal of Petrology, 3 (1962) 342-532.

[17] E. Kazemi-Khasragh, F. Bahari-Sambran, S.M.H. Siadati, R. Eslami-Farsani, S. Arbab Chirani, The effects of surface-modified graphene nanoplatelets on the sliding wear properties of basalt fibers-reinforced epoxy composites, Journal of Applied Polymer Science, (2019) 47986.

[18] D.S. Achilias, M.M. Karabela, E.A. Varkopoulou, I.D. Sideridou, Cure kinetics study of two epoxy systems with fourier tranform infrared spectroscopy (FTIR) and differential scanning calorimetry (DSC), Journal of Macromolecular Science, Part A, 49 (2012) 630-638.

[19] A. Mirmohseni-Namin, S. Nikafshar, F. Mirmohseni, Increasing toughness and tensile strength of an epoxy–diamine system using an inorganic ultra-accelerator, RSC Advances, 5 (2015) 53025-53035.

[20] H. Zhang, S. Gn, J. An, Y. Xiang, J. Yang, Impact behaviour of GLAREs with MWCNT modified epoxy resins, Experimental Mechanics, 54 (2014) 83-93.

[21] H. Khoramishad, H. Alikhani, S. Dariushi, An experimental study on the effect of adding multi-walled carbon nanotubes on high-velocity impact behavior of fiber metal laminates, Composite Structures, 201 (2018) 561-569.

[22] X. Zhang, Y. Hu, H. Li, J. Tian, X. Fu, Y. Xu, Y. Lu, Y. Chen, L. Qin, J. Tao, Effect of multi-walled carbon nanotubes addition on the interfacial property of titanium-based fiber metal laminates, Polymer Composites, 39 (2018) E1159-E1168.

[23] Z. Asaee, M. Mohamed, S. Soumik, F. Taheri, Experimental and numerical characterization of delamination buckling behavior of a new class of GNP-reinforced 3D fiber-metal laminates, Thin-Walled Structures, 112 (2017) 208-216.

[24] A.Z. Zakaria, K. Shelesh-nezhad, Introduction of nanoclay-modified fiber metal laminates, Engineering Fracture Mechanics, 186 (2017) 436-448.

[25] A. Kinloch, A. Taylor, The mechanical properties and fracture behaviour of epoxy-inorganic micro-and nano-composites, Journal of Materials Science, 41 (2006) 3271-3297.

[26] B. Qi, Q. Zhang, M. Bannister, Y.-W. Mai, Investigation of the mechanical properties of DGEBA-based epoxy resin with nanoclay additives, Composite Structures, 75 (2006) 514-519.

[27] R.M. Moghadam, S. Saber-Samandari, S.A. Hosseini, On the tensile behavior of clay–epoxy nanocomposite considering interphase debonding damage via mixed-mode cohesive zone material, Composites Part B: Engineering, 89 (2016) 303-315.

[28] O. Zabihi, M. Ahmadi, S. Nikafshar, K.C. Preyeswary, M. Naebe, A technical review on epoxy-clay nanocomposites: Structure, properties, and their applications in fiber reinforced composites, Composites Part B: Engineering, (2017).

[29] D. Paul, L.M. Robeson, Polymer nanotechnology: nanocomposites, Polymer, 49 (2008) 3187-3204.

[30] O. Zabihi, H. Khayyam, B.L. Fox, M. Naebe, Enhanced thermal stability and lifetime of epoxy nanocomposites using covalently functionalized clay: experimental and modelling, New Journal of Chemistry, 39 (2015) 2269-2278.

[31] R.E. Farsani, S. Khalili, V. Daghigh, Charpy impact response of basalt fiber reinforced epoxy and basalt fiber metal laminate composites: Experimental study, International Journal of Damage Mechanics, 23 (2014) 729-744.

[32] L. Ferrante, F. Sarasini, J. Tirillò, L. Lampani, T. Valente, P. Gaudenzi, Low velocity impact response of basalt-aluminium fibre metal laminates, Materials & Design, 98 (2016) 98-107.

[33] F. Bahari-Sambran, R. Eslami-Farsani, S. Arbab Chirani, The flexural and impact behavior of the laminated aluminum-epoxy/basalt fibers composites containing nanoclay: An experimental investigation, Journal of Sandwich Structures & Materials, (2018) 1099636218792693.

[34] H. Aghamohammadi, S.N.H. Abbandanak, R. Eslami-Farsani, S.H. Siadati, Effects of various aluminum surface treatments on the basalt fiber metal laminates interlaminar adhesion, International Journal of Adhesion and Adhesives, 84 (2018) 184-193.

[35] M.E. Mehr, H. Aghamohammadi, S.H. Abbandanak, G.R. Aghamirzadeh, R. Eslami-Farsani, S. Siadati, Effects of applying a combination of surface treatments on the mechanical behavior of basalt fiber metal laminates, International Journal of Adhesion and Adhesives, 92 (2019) 133-141.

[36] Z. Fan, M.H. Santare, S.G. Advani, Interlaminar shear strength of glass fiber reinforced epoxy composites enhanced with multi-walled carbon nanotubes, Composites Part A: Applied science and manufacturing, 39 (2008) 540-554.

[37] Y.-J. Wan, L.-C. Tang, L.-X. Gong, D. Yan, Y.-B. Li, L.-B. Wu, J.-X. Jiang, G.-Q. Lai, Grafting of epoxy chains onto graphene oxide for epoxy composites with improved mechanical and thermal properties, Carbon, 69 (2014) 467-480.

[38] S. Zeng, M. Shen, Y. Xue, Y. Zheng, K. Zhang, Y. Han, L. Yang, Controllable mechanical properties of epoxy composites by incorporating self-assembled carbon nanotube–montmorillonite, Composites Part B: Engineering, 164 (2019) 368-376.

[39] W. Liu, S.V. Hoa, M. Pugh, Organoclay-modified high performance epoxy nanocomposites, Composites Science and Technology, 65 (2005) 307-316.

[40] G. Withers, Y. Yu, V. Khabashesku, L. Cercone, V. Hadjiev, J. Souza, D. Davis, Improved mechanical properties of an epoxy glass–fiber composite reinforced with surface organomodified nanoclays, Composites Part B: Engineering, 72 (2015) 175-182.

This is the accepted manuscript (postprint) of the following article:
Bahari-Sambran, F., Meuchelboeck, J., Kazemi-Khasragh, E., Eslami-Farsani, R., & Chirani, S. A. (2019). The effect of surface modified nanoclay on the interfacial and mechanical properties of basalt fiber metal laminates. *Thin-Walled Structures*, *144*, 106343.
https://doi.org/10.1016/j.tws.2019.106343

[41] Y. Xu, S. Van Hoa, Mechanical properties of carbon fiber reinforced epoxy/clay nanocomposites, Composites Science and Technology, 68 (2008) 854-861.

[42] M.H. Pol, G. Liaghat, Investigation of the high velocity impact behavior of nanocomposites, Polymer Composites, 37 (2016) 1173-1179.

[43] A. Arifin, S. Abdullah, M. Rafiquzzaman, R. Zulkifli, D.A. Wahab, A. Arifin, Investigation of the behaviour of a chopped strand mat/woven roving/foam-Klegecell composite lamination structure during Charpy testing, Materials & Design, 59 (2014) 475-485.

[44] H. Khosravi, R. Eslami-Farsani, Enhanced mechanical properties of unidirectional basalt fiber/epoxy composites using silane-modified Na+-montmorillonite nanoclay, Polymer Testing, 55 (2016) 135-142.

[45] G. Wu, J.-M. Yang, The mechanical behavior of GLARE laminates for aircraft structures, Jom, 57 (2005) 72-79.